Atmos. Chem. Phys., 14, 10145–10162, 2014
www.atmos-chem-phys.net/14/10145/2014/
doi:10.5194/acp-14-10145-2014

Atmospheric Chemistry and Physics
Open Access

Chemical mass balance of 300 °C non-volatile particles at the tropospheric research site Melpitz, Germany

L. Poulain[1], W. Birmili[1], F. Canonaco[2], M. Crippa[2], Z. J. Wu[1], S. Nordmann[1,*], G. Spindler[1], A. S. H. Prévôt[2], A. Wiedensohler[1], and H. Herrmann[1]

[1]Leibniz-Institute for Tropospheric Research (TROPOS), Permoserstr. 15, 04318 Leipzig, Germany
[2]Laboratory of Atmospheric Chemistry, Paul Scherrer Institute (PSI), 5232 Villigen, Switzerland
[*]now at: Max Planck Institute for Chemistry, Hahn-Meitner-Weg 1, 55128 Mainz, Germany

Correspondence to: L. Poulain (poulain@tropos.de)

Received: 7 August 2013 – Published in Atmos. Chem. Phys. Discuss.: 16 October 2013
Revised: 17 August 2014 – Accepted: 18 August 2014 – Published: 23 September 2014

Abstract. In the fine-particle mode (aerodynamic diameter < 1 µm) non-volatile material has been associated with black carbon (BC) and low-volatile organics and, to a lesser extent, with sea salt and mineral dust. This work analyzes non-volatile particles at the tropospheric research station Melpitz (Germany), combining experimental methods such as a mobility particle-size spectrometer (3–800 nm), a thermodenuder operating at 300 °C, a multi-angle absorption photometer (MAAP), and an aerosol mass spectrometer (AMS). The data were collected during two atmospheric field experiments in May–June 2008 as well as February–March 2009. As a basic result, we detected average non-volatile particle–volume fractions of 11 ± 3 % (2008) and 17 ± 8 % (2009). In both periods, BC was in close linear correlation with the non-volatile fraction, but not sufficient to quantitatively explain the non-volatile particle mass concentration. Based on the assumption that BC is not altered by the heating process, the non-volatile particle mass fraction could be explained by the sum of black carbon (47 % in summer, 59 % in winter) and a non-volatile organic contribution estimated as part of the low-volatility oxygenated organic aerosol (LV-OOA) (53 % in summer, 41 % in winter); the latter was identified from AMS data by factor analysis. Our results suggest that LV-OOA was more volatile in summer (May–June 2008) than in winter (February–March 2009) which was linked to a difference in oxidation levels (lower in summer). Although carbonaceous compounds dominated the sub-µm non-volatile particle mass fraction most of the time, a cross-sensitivity to partially volatile aerosol particles of maritime origin could be seen. These marine particles could be distinguished, however from the carbonaceous particles by a characteristic particle volume–size distribution. The paper discusses the uncertainty of the volatility measurements and outlines the possible merits of volatility analysis as part of continuous atmospheric aerosol measurements.

1 Introduction

Atmospheric aerosol particles are made of a large variety of organic and inorganic compounds. They affect global climate through direct and indirect radiative forcing (IPCC, 2007), the ecosystem (e.g., Bohlmann et al., 2005; Jickells et al., 2005; Molina and Molina, 2004) as well as human health (e.g., Gurjar et al., 2010; Ostro et al., 2007; Pope, 2000). Moreover, aerosol chemistry and thermodynamic properties (e.g., heterogeneous interactions and chemistry, condensation or evaporation of semi-volatile compounds on the particle phase) directly contribute to modify the chemical composition of both atmospheric gas and particle phases (e.g., Kolb and Worsnop, 2012; Pöschl et al., 2007). In a worldwide overview of sub-µm chemical particle composition, Zhang et al. (2007) reported organic mass fractions between 20 and 90 % in PM_1 depending on location and season. This organic fraction is difficult to characterize because it includes thousands of organic compounds, many of which have not been identified analytically. Organic aerosol particles are of biogenic and/or anthropogenic origin and can be emitted directly from these sources (primary organic aerosol – POA), or formed as a secondary organic aerosol (SOA) by chemical

reactions of gas phase precursors such as volatile organic compounds (VOCs) to form low volatility reaction products which can partition into particles (e.g., Kanakidou et al., 2005; Hallquist et al., 2009). The aerosol particle composition is strongly depending on the gas-to-particle partitioning of their constitutive compounds.

In studies related to the atmosphere, volatility analysis has proved to be useful to differentiate classes of inorganic compounds, such as particulate ammonium nitrate, ammonium sulfate, sulfuric acid, and sodium chloride (Schmid et al., 2002; Smith and O'Dowd, 1996). After the evaporation of high-volatile particulate compounds, volatility analysis leaves non-volatile particle cores containing material that is non-volatile at the given temperature. Hence, the volatilization temperature is, among others, a parameter that can be characteristic for certain classes of organic, but also inorganic compounds. In the fine-particle mode (aerodynamic diameter < 1 µm), non-volatile material has been associated with black carbon particles and low-volatile organic, and to a lesser extent with sodium chloride and crustal material (e.g., Engler et al., 2007; Huffman et al., 2008, 2009). While the volatilization temperatures of inorganic compounds are relatively well known (cf. Engler et al., 2007), there are more uncertainties for the organic phase; the ratio of more and less volatile compounds, in particular, strongly depends on the source of the particulate matter, and the stage of the aerosol within its atmospheric lifecycle. For example, the chemical composition as well as the thermodynamic properties of SOA are not constant over time but evolve during the aging processes of the aerosol (e.g., Donahue et al., 2012a). Therefore, Donahue et al. (2006) developed the volatility basis set (VBS) approach, a model where organic aerosols formation and aging processes is described by their saturation vapor pressure (C^*). SOA volatility depends on the cascade of reactions that happen during the aging processes, with functionalization leading to compounds with lower volatility, and fragmentation contributing to a higher volatility (Jimenez et al., 2009). A quantitative relationship between C^* and the organic aerosol oxidation state was introduced in an improved VBS model (2D-VBS, Donahue et al., 2011, 2012b).

A practical device to investigate aerosol particle volatility is the thermodenuder (TD). Here, aerosol particles are evaporated in the airborne state inside a heated flow tube at defined temperature. See Burtscher et al. (2001) for a survey of the design of different TDs. The TD can, in principle, be combined with most particle sampling techniques and online particle sizing and classification instruments. Volatility tandem differential mobility analyzers (V-TDMA; Rose et al., 2006; Philippin et al., 2004) have been used to measure the shrinkage of monodisperse particles after volatilization. The volatility twin differential mobility particle sizer (V-TDMPS; V-SMPS), in contrast, measures complete particle number–size distributions upstream and downstream of the TD (Ehn et al., 2007; Engler et al., 2007). Comparing integral particle properties such as number and volume upstream and downstream of a TD allows estimating the non-volatile fraction at the given temperature. In order to investigate the non-volatile part of atmospheric aerosol particles on a long-term basis, continuous V-TDMPS or V-SMPS measurements have been implemented at several atmospheric observation sites in Germany: the rural research site Melpitz (Engler et al., 2007), the HGMU urban monitoring site Augsburg (Birmili et al., 2010), and six other stations inside the German Ultrafine Aerosol Network (GUAN; Birmili et al., 2009). In all cases, a temperature of 300 °C was selected in the thermodenuder. The reason for choosing this temperature is that sulfates, nitrates and most organic compounds would be stripped off while the charring of organic matter would be prevented in the presence of atmospheric oxygen (cf. Engler et al., 2007).

The motivation to monitor black carbon and other non-volatile particle compounds in atmospheric networks involves, on the one hand, the necessity to help quantify the regional and global effect of light absorption (Cheng et al., 2009; Koch et al., 2009; Stier et al., 2007; Bond and Bergstrom, 2006). On the other hand, atmospheric soot particles and non-volatile compounds have been associated with certain adverse health effects by epidemiological and toxicological studies (Attfield et al., 2012; Janssen et al., 2012; Mazzarella et al., 2007; Totlandsdal et al., 2012). A monitoring strategy such as that pursued in GUAN attempts to provide experimental data that can be used to address both issues mentioned above. As an additional issue, volatility instruments have also been used to examine the evolution of the atmospheric nucleation mode. A substantial observation has been that each particle of the evolving atmospheric nucleation mode seems to contain a non-volatile core at 300 °C, even though these particles were initially formed purely from gas-to-particle conversion at ambient temperatures (Ehn et al., 2007; Wehner et al., 2005).

Recently, an aerosol mass spectrometer (AMS, e.g., Canagaratna et al., 2007) was combined with the TD, allowing a direct investigation of the chemical composition of the non-volatile fraction (Faulhaber et al., 2009; Huffman et al., 2008, 2009; Wu et al., 2009). These measurements point out that the non-volatile fraction is not only made of black carbon and crustal material (which cannot be detected by the AMS), even at temperatures higher than 200 °C, but that the presence of a non-volatile organic fraction has to be considered as well. These remaining organic compounds represent an important description parameter for a better estimation of the atmospheric organic aerosol (OA) since it should be only negligibly influenced by dilution and gas-to-particle equilibrium. Improving our understanding on this low-volatile organic fraction is necessary in order to improve the current SOA models, to better estimate the impact of the OA to the global aerosol mass loading and to finally better predict the organic contribution to both climate and human health.

In this study, a mass closure study based on parallel TD, AMS, and MAAP measurements to identify the composition of non-volatile fraction at 300 °C during two intensive

campaigns in May–June 2008 and February–March 2009 at the TROPOS Central European regional atmospheric research station Melpitz (Germany) is performed. A simple method will be used to estimate the non-volatile chemical composition, principally based on laboratory measurements performed using a similar TD running in comparable conditions as well as on comparisons with similar measurements available in the literature. The influence of the meteorological conditions as well as of the air mass origin on the non-volatile fraction will be discussed.

2 Experimental

2.1 The TROPOS research station Melpitz (Germany)

Atmospheric aerosol measurements were performed at the TROPOS research station Melpitz (51.54° N, 12.93° E, 86 m a.s.l.), 50 km to the north-east of Leipzig, Germany. The station has been used since 1992 to examine the effect of atmospheric long-range transport on local air quality. The site itself is mainly surrounded by agricultural pastures and forests. The atmospheric aerosol observed at Melpitz can be regarded as representative for Central European regional conditions, as confirmed by multiple site comparisons within the program EMEP: Co-operative Programme for monitoring and evaluation of the long-range transmissions of air pollutants in Europe (Aas et al., 2012) and the GUAN Network (Birmili et al., 2009).

All online instruments were set up in the same container laboratory and utilized the same air inlet. This inlet line consisted of a PM_{10} Anderson impactor located approximately 6 m above ground level and directly followed by an automatic aerosol diffusion dryer to keep the relative humidity inside the sampling line below 30 % (Tuch et al., 2009). After entering the container laboratory, the sampling flow was divided among the different instruments. For a basic overview of the physical and chemical aerosol characterization methods see, e.g., Birmili et al., 2008 and Spindler et al., 2010, 2012, 2013).

2.2 Chemical particle composition

2.2.1 AMS

The AMS is an Aerodyne high-resolution time-of-flight aerosol mass spectrometer (HR-ToF-AMS) here simply referred to as AMS (DeCarlo et al., 2006). Briefly, the AMS allows two alternative detection modes to measure the particle-size distribution (particle time-of-flight (PToF) mode) and the chemical composition of the particle (mass spectrum (MS) mode). Before being detected by the time-of-flight mass spectrometer, the particles are flash vaporized by impaction on a heated surface (600 °C) and the vapors are ionized by an electron impact ionization source at 70 eV. Because soot, crustal material, and sea salt can usually not be properly detected and quantify by the AMS, while Ovadnevaite et al. (2012) demonstrated the possibility to measure sea salt, the AMS is commonly considered to only provide non-refractory PM_1 aerosol chemical composition. Different AMS intercomparison exercises (performed by Bahreini et al., 2009, Crippa et al., 2013 and Freutel et al., 2013) estimated the total AMS variability around 30 % (including 10 % for the different inlets, 20 % for the ionization efficiency calibration, and 20 % for the bounce efficiency). Further details on the AMS data analysis and results for these two measurements periods can be found in Poulain et al. (2011).

Source apportionment of the organic aerosol fraction was conducted using the unit mass resolution (UMR) organic mass spectra and performed using the multi-linear engine algorithm (ME-2) developed by Paatero (1999). Its results were analyzed according to the ME-2 graphic interphase developed by the Paul Scherrer Institute and detailed in Canonaco et al. (2013). Further details on the factor analysis results can be found in Crippa et al. (2014).

2.2.2 MAAP

The black carbon (BC) mass concentration was estimated by a multi-angle absorption photometer (MAAP, Model 5012, Thermo-scientific, Petzold and Schönlinner, 2004). This instrument internally converts the absorption coefficient measured at a wavelength of 637 nm to the soot mass concentration by applying a constant mass absorption coefficient of $6.6\,m^2\,g^{-1}$. This value was determined from a combination of independent measurements of the absorption coefficient using the MAAP and the soot mass concentration applying a thermographic method for urban aerosol samples (Petzold and Schönlinner, 2004). However, model calculations and experimental literature results suggest that the mass absorption coefficient of atmospheric soot particles is not constant, but may depend on the state of mixture with other compounds (Fuller et al., 1999). The analysis of graphitic carbon from MAAP filter samples at various GUAN sites using Raman-spectroscopy yielded an average mass absorption efficiency of $5.3\,m^2\,g^{-1}$ for Germany (Nordmann et al., 2013), which differs from the default mass absorption efficiency of $6.6\,m^2\,g^{-1}$. Although this value appears to be more accurate that the default value; it cannot exclude the fluctuations of this coefficient during measurements due to the present of other absorbing compounds. However, this implies a systematic uncertainty of BC derived from the MAAP measurements, depending on which mass absorption efficiency is used.

An additional source of error is the measurement accuracy of an individual MAAP instrument. Direct intercomparison of multiple MAAP instruments yielded a variability of less than 5 % around the mean value (Müller et al., 2011). Another correction was necessary in this work: at Melpitz, the MAAP is operated downstream of a PM_{10} inlet. Our subsequent calculations, however, refer to PM_1. We

converted BC (PM_{10}) to BC (PM_1) by multiplication with a factor of 0.9, which was obtained by running two MAAPs at Melpitz side by side with different inlets (cf. Poulain et al., 2011). Considering instrumental, mass absorption efficiency, density and size cutting uncertainties, a global uncertainty of approximately 15 % on the PM_1 BC mass concentration can be expected.

2.3 Ambient and non-volatile particle number–size distributions

Particle number–size distributions (3–800 nm) were continuously measured upstream and downstream of a TD using a volatility twin differential mobility particle sizer (V-TDMPS). The TD follows the design of Wehner et al. (2002). Briefly, it consists of a heating section (50 cm) followed by a cooling section filled with active carbon to remove evaporated material and to cool down the sample to room temperature. The TD was used at a flow rate between 2.5 and 3.0 L min^{-1} (corresponding to a residence time on the heating section of approximately 3.8 and 3.1 s, respectively) and at a constant temperature of 300 °C. The working temperature is considered, on the one hand, to be high enough for evaporating the most important parts of the inorganic ions (especially ammonium nitrate and ammonium sulfate) as well as most organic carbon and, on the other hand, as a temperature low enough to prevent charring of organic compounds.

A twin differential mobility particle sizer (TDMPS, Birmili et al., 1999) was deployed to measure particle number–size distributions from 3–800 nm mobility diameter with a time resolution of 10 min, changing its sampling inlet between atmosphere aerosol and this aerosol after passing through the thermodenuder. The system consisted of two differential mobility analyzers (DMA, Hauke-type) and two condensation particle counters (CPC, TSI model 3010 and TSI model 3025). The sheath air was circulated in closed loops for both DMAs. The evaluation of particle number–size distributions includes a multiple charge inversion, the CPC efficiency and diffusional losses in the DMA, and all internal and external sampling lines according to the recommendations in Wiedensohler et al. (2012). The V-TDMPS data was additionally corrected for particle losses due to diffusion inside the TD. The particle volume concentrations are calculated from the measured number size distribution assuming spherical particles. The volume fraction remaining (VFR) was determined by dividing the non-volatile volume concentration measured downstream of the TD by the total particle volume measured at ambient temperature, i.e., bypassing the TD.

2.4 Off-line chemical characterization

During the 2008 campaign, daily $PM_{2.5}$ high volume DIGITEL filter samples (Digitel Elektronic AG, Hegnau, Switzerland) were collected from midnight to midnight, while during the 2009 campaign, daily PM_1 high volume DIGITEL filter samples were taken. A 5-stage BERNER impactor (Hauke, Austria; Berner and Lurzer, 1980) was deployed on individual days (from midnight to midnight) during February–March 2009. All filters were analyzed according to the same analytical methods. Filters were weighted for the total particle mass and water soluble inorganic cations and anions as well as organic carbon (OC) and elemental carbon (EC) were determined. Details on the different analytical methods and results for these two specific periods can be found in Spindler et al. (2010). Water insoluble ions, dust, and metals were not measured and consequently contribute to the non-explained mass fraction of filters. On averaged, a mass recovery of around 82 % was obtained for the PM_1 filters during winter time and 62 % for the $PM_{2.5}$ filters during summer time. The lower recoveries value of the $PM_{2.5}$ filters compared to the PM_1 might be attributed to a larger contribution of crustal materials in the $PM_{2.5}$ size range compared to the one in PM_1

3 Results

3.1 Mass closure

Before discussing the volatility measurements, the balance of PM_1 particle mass obtained from AMS and MAAP on the one hand, and the TDMPS on the other hand is examined. To convert the particle volume concentration from the TDMPS into a mass concentration, we estimated the gravimetric particle density on the basis of measured chemical composition using Eq. (1) (Salcedo et al., 2006). In this equation, the density of ammonium nitrate and ammonium sulfate was assumed to be 1.75 g cm^{-3} (Lide, 1991), the density of ammonium chloride as 1.52 g cm^{-3} (Lide, 1991), the density of organic matter as 1.2 g cm^{-3} (Turpin and Lim, 2001), and the density of BC as 1.77 g cm^{-3} (Park et al., 2004). A discussion on the density of BC can be found in Sect. S1 in the Supplement.

$$\text{density} = \frac{[\text{Total}_{\text{AMS}} + \text{BC}]}{\frac{[NO_3^-]+[SO_4^{2-}]+[NH_4^-]}{1.75} + \frac{[Cl^-]}{1.52} + \frac{[\text{Org}]}{1.2} + \frac{[\text{BC}]}{1.77}} \quad (1)$$

Applying the density to measured particle composition, a mean density of 1.4 g cm^{-3} for May–June 2008 and 1.6 g cm^{-3} for February–March 2009 was obtained, respectively. The reconstructed mass concentrations are presented in Fig. 1 and show a reasonable linear correlation coefficient (r Pearson) with $r = 0.95$ in 2008, and $r = 0.94$ in 2009.

It needs to be noted that the mass concentrations derived from the TDMPS are on average 20 % higher than those

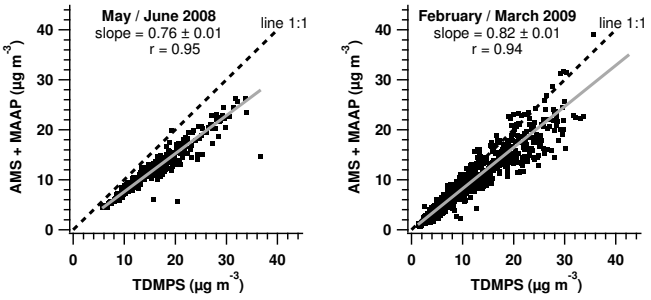

Figure 1. Measured AMS + MAAP mass concentration vs. TDMPS estimated mass concentration for May–June 2008 (left) and February–March 2009 (right) periods. Estimation of the TDMPS mass concentration was made using Eq. (1). Correlation curves were calculated using the least orthogonal distance fit method

derived from AMS and MAAP (Fig. 1) which is close to previous comparisons (e.g., Mensah et al., 2012; Setyan et al., 2012). This deviation is within the range of instrumental uncertainties provided by the methods used: TDMPS total particle volume (± 10 %), BC PM_1 mass concentration (15 %), AMS mass concentrations (30 %), and density estimation. In addition, another source of uncertainties related to the different size cut offs of the AMS and TDMPS has to be considered. The transmission efficiency of the AMS aerodynamic lenses starts decreasing towards 700 nm (mobility), so that the mass concentration of non-refractory compounds measured by the AMS might underestimate the one measured by the TDMPS (upper size range 800 nm mobility). Differences due to different amounts of water present in the particulate phase as a result of particle hygroscopicity can be neglected because the relative humidity in the sample aerosol was always below 30 %.

3.2 Ambient and non-volatile particle volume concentrations

Figure 2 shows the time series of the ambient and non-volatile particle volume concentrations obtained from the TDMPS, in conjunction with the VFR at 300 °C. The VFR is higher in the February–March 2009 period (17 ± 8 %; mean ± standard deviation) compared to the May–June 2008 period (11 ± 3 %). It can also be seen that the VFR shows considerable variations with time, although to a lesser extent than the total particle volume concentrations. Such seasonality may be due to a change in the aerosol chemical composition as discussed in the following sections. In order to directly compare the non-volatile particle volume concentration (NVVC) measured after the TD with the aerosol chemical composition, it is essential to convert it into non-volatile mass concentration (NVMC). As discussed above, the particle density directly depends on its chemical composition. However, in contrary to ambient particles, the chemical composition of the non-volatile fraction is unknown. Therefore,

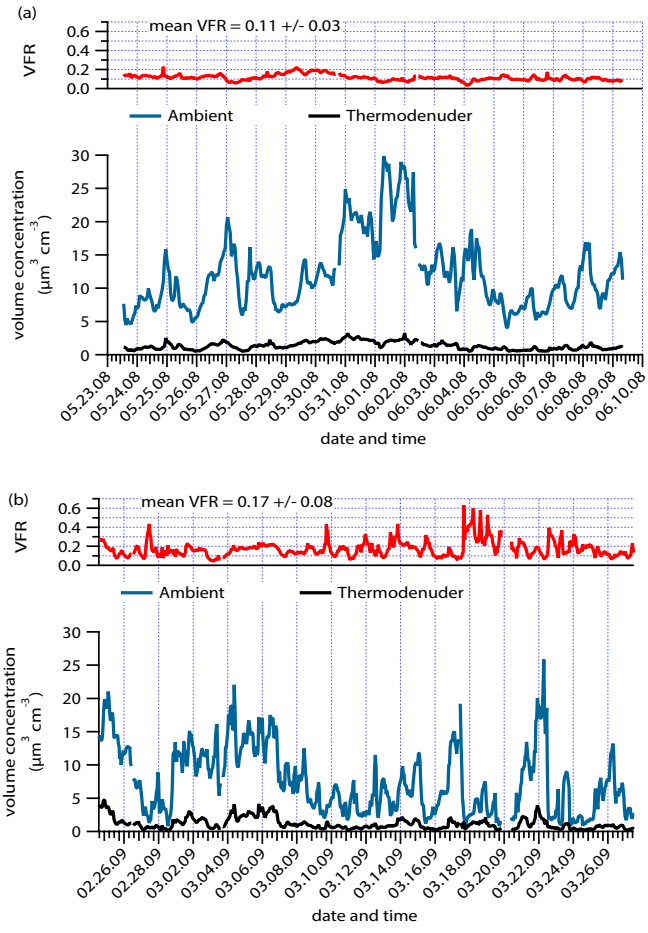

Figure 2. Time series of the ambient and non-volatile volume concentration measured during May–June 2008 **(a)** and February–March 2009 **(b)** periods. The volume fraction remaining (VFR) for each time period is also presented on the top panel of each plot, including the mean value (± 1σ) for each measurement period.

in the following, a constant density of 1.6 g cm^{-3} was applied to convert the TD measurements into mass concentration.

3.2.1 Black carbon contribution to the non-volatile mass concentration

Black carbon is considered a major non-volatile component in sub-µm PM (e.g., Pöschl, 2005). During the GUAN project, Birmili et al. (2009) found linear relationships between the BC mass concentrations and the non-volatile volume concentrations for five different atmospheric measurement sites. It is therefore a strong hypothesis that BC constitutes a major part of the non-volatile mass concentration.

Detailed correlations between non-volatile particles and BC are shown in Fig. 3a and c. The correlations between the calculated non-volatile particle mass concentration and the BC concentration yield slopes well below 1, as well as correlations (r) of 0.93 (May–June 2008) and 0.90 (February–March 2009). Similar slopes were obtained for the 2008

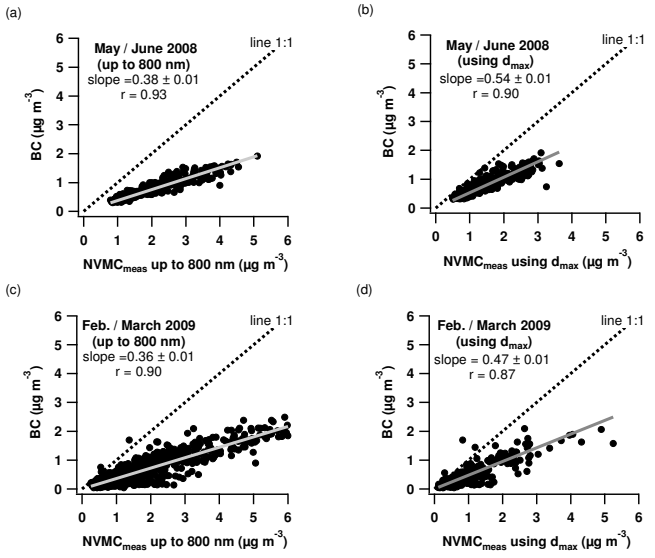

Figure 3. Black carbon (BC) vs. the non-volatile mass concentration (NVMC) estimated from the TDMPS for May–June 2008 and February–March 2009 periods. Estimation of the non-volatile mass concentration was made assuming a density of 1.6 g cm^{-3}. The left panels correspond to the total V-TDMPS size range (up to 800 nm) while the right panels refer to a time-dependent upper size cutting ($d_{\max}$). Correlation curves were calculated using the least orthogonal distance fit method.

(0.38) and 2009 (0.36) periods. These results confirmed that BC alone cannot explain the entire non-volatile mass fraction.

3.2.2 Inorganic contribution to the non-volatile mass concentration

In the continental troposphere, the inorganic sub-µm particulate fraction consists of major amounts of ammonium nitrate and ammonium sulfate. This was confirmed for Melpitz by Poulain et al. (2011). Ammonium nitrate is a semi-volatile compound that starts evaporating at 30 °C, while ammonium sulfate is a less volatile compound, evaporating only at around 150 °C from the particulate phase in a thermodenuder of our type (Wu et al., 2009). In real environment, particle composition is much more complex than pure standards; therefore, evaporation of inorganic salts in internally mixed particles might slightly differ from that of pure salts (Huffman et al., 2009). However, Huffman et al. (2009) reported only a residual mass fraction remaining of nitrate and sulfate at 250 °C slightly below 10 % which cannot be clearly attributed to either inorganic salts from internally mixed particles that did not fully evaporated or non-volatile organosulfate/organonitrate compounds. Consequently, at 300 °C, contribution of ammonium nitrate and sulfate are expected to be quite negligible (< 10 %).

It can be thought that other inorganic compounds, such as chloride, sodium, calcium, potassium, or magnesium remain in the particulate phase at 300 °C. However, their concentrations were rather low compared to the concentrations of ammonium sulfate and nitrate, as suggested by DIGITEL filter samples taken simultaneously with our study (Daily $PM_{2.5}$ filter samples were taken during May–June 2008, while daily PM_1 filter samples were taken during February–March 2009). Specifically, chloride, sodium, calcium, potassium, and magnesium accounted for around 8 % of the total identified inorganic $PM_{2.5}$ concentration and for around 4 % of the identified inorganic PM_1 mass (Poulain et al., 2011; Spindler et al., 2010).

3.2.3 Organic contribution to the non-volatile mass concentration

In this section, we discuss the possible organic contribution to the NVMC, based on the AMS measurements. Figure 4 illustrates the mass balance for the non-volatile particle mass, which is described in detail in the following.

As described in Sect. 2.2.1., factor analysis of organic aerosol matter was performed using the ME-2 approach to describe the organic aerosols. A detailed description of the ME-2 analysis can be found in Crippa et al. (2014) and is summarized in Sect. S2 in the Supplement. Only the main results will be discussed here. In May–March 2008, three factors were identified to explain the total organic aerosol (OA). These factors correspond to low-volatility oxygenated organic aerosol (LV-OOA, 46.7 % of total OA), semi-volatile oxygenated organic aerosol (SV-OOA, 45.7 % of total OA) and hydrocarbon-like organic aerosol (HOA, 7.5 % of total OA). In February–March 2009, an additional factor was found, and identified as biomass burning emissions (biomass burning organic aerosol or BBOA, 13.3 % of total OA). During this period, LV-OOA, SV-OOA, and HOA represent 43.4, 32.9, and 10.3 % of total OA, respectively. HOA and BBOA are related to primary organic aerosol sources: BBOA represents biomass burning while the HOA is more related to traffic and liquid domestic fuel combustion. LV-OOA and SV-OOA are more related to secondary organic aerosol. LV-OOA is known to be associated with more oxygenated OA with the lowest volatility, while the SV-OOA is commonly considered to be representative for freshly generated OA made of less oxygenated OA, with a higher volatility than LV-OOA (e.g., Jimenez et al., 2009; Lanz et al., 2007; Ulbrich et al., 2009).

Previous field measurements, using a coupled TD–AMS setup (Huffman et al., 2009) demonstrated that similar factor analysis components and time series results were observed when comparing ambient only PMF results with joint ambient-TD results. Therefore, it seems to be possible to extrapolate the non-volatile fraction at a specific temperature from the ambient PMF factors when their MFR at this temperature are known. The same authors reported that at

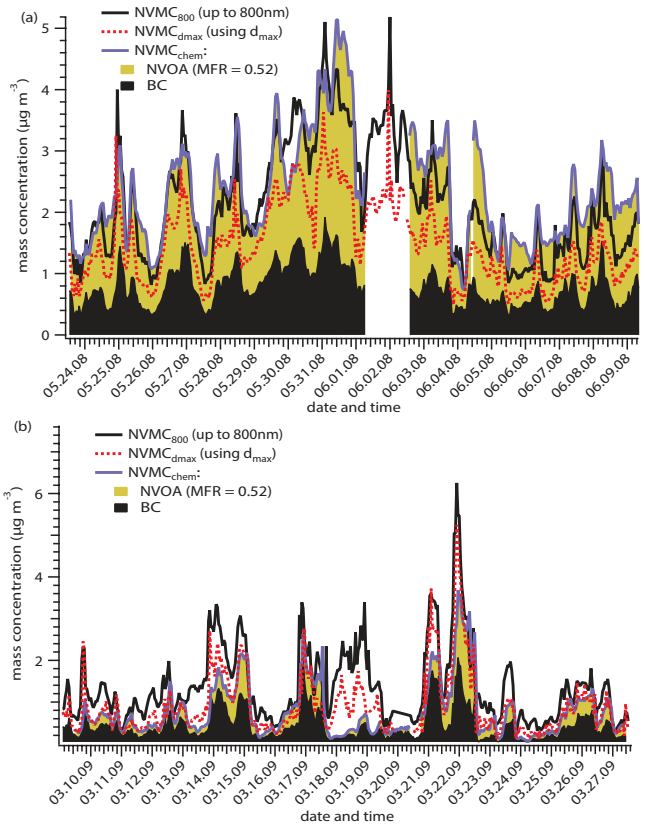

Figure 4. Time series of the estimated non-volatile OA (NVOA) and BC for **(a)** May–June 2008 and **(b)** February–March 2009. Time series of the resulting estimated and measured non-volatile mass concentration (NVMC) are included as blue and black solid lines, respectively. The V-TDMPS results were converted in mass concentration assuming a constant density of 1.6 g cm^{-3}. The red dotted lines correspond to NVMC measured with a time-dependent upper size cutting d_{max} (see discussion in Sect.3.4.1).

250–270 °C, SV-OOA, HOA, and BBOA nearly fully evaporated (with a mass fraction remaining (MFR) near or below 10 %), while LV-OOA presents a MFR of 70–30 %, depending on the location. Because LV-OOA has a similar mass spectrum as humic-like substances (HULIS), Wu et al. (2009) investigated the temperature dependency of the volatility of fulvic and humic acids as surrogate for HULIS, using a similar TD–AMS setup as in the present study. Within that study it was found that these two compounds present a MFR of 47 % for fulvic acid and 58 % for humic acid after being heated at 300 °C, in agreement with the field observations made by Huffman et al. (2009). Additionally, changes of the mass spectra of the fulvic and humic acids at 300 °C compared to the ambient mass spectra were attributed to the loss of water molecule and decarboxylation. Kondo et al. (2011) reported an evaporation of 10–30 % for laboratory generated monodisperse particles of different surrogates of atmospheric HULIS heated at 300 °C and 400 °C with a residence time inside the heated part of 0.3 s. Although direct comparisons between the different TD measurement can be strongly influenced by the residence time of the particle inside the heated section (An et al., 2007), the previous works are in good agreement and confirm that a large fraction of the HULIS are not evaporated even after being heated at high temperatures.

Since Wu et al. (2009) used the same TD setup as in the present work, the non-volatile organic aerosol (NVOA) mass concentration was estimated to represent 52 % of the measured LV-OOA, which is the mean value of the measured surrogate of HULIS used by the authors. This is also in agreement with the mean value of the Huffman et al. (2009) observations.

Time series of the estimated NVOA fraction for each season are presented in Fig. 4 and the relationship with the measured non-volatile mass concentration is shown in Fig. S3 in the Supplement. The relationship between NVOA and the measured non-volatile mass shows a correlation slope of 0.74 ($r = 0.71$) and 0.24 ($r = 0.58$) for 2008 and 2009, respectively (Fig. S3a, d). These results will be discussed in the following.

3.3 Assessment of the non-volatile particles chemical composition

Figures 4 and 5 illustrate the time series and inter-parameter correlations of BC, non-volatile OA, and the non-volatile mass concentration (NVMC) derived from the V-TDMPS. Overall, the May–June 2008 period exhibits higher mass concentrations than the February–March 2009 period. In both periods, the NVMC proves to be highly variable on the scale of hours. A look at the time series of NVMC estimated from AMS/MAAP and measured by the V-TDMPS shows a significant covariance, down to the timescale of hours, although the mean values do not coincide during all periods.

The good correlation (slope of 1.11, $r = 0.88$) during May–June 2008 indicates that the measured non-volatile fraction at 300 °C can be quantitatively explained by BC and non-volatile OA (Fig. 5a). In this case, the non-volatile OA represents 66 ± 8 % of the reconstructed non-volatile mass. In contrast, only 60 % of the measured non-volatile mass during February–March 2009 can be explained by the same approach (Figs. 4 and 5d). In that second case, the non-volatile OA represents 41 ± 13 % of the reconstructed non-volatile mass.

It should be noted that the discrepancy between estimated and measured NVMC was not constant over the whole measurement period in February–March 2009. On some days the balance was matched (e.g., 16, 17, 25, 26, and 27 March), while on others a large discrepancy could be observed (e.g., 18–19 March, 2009, and the first days of the measurement period). Interestingly, the largest differences usually occurred when particles consisted of a particularly large non-volatile fraction (Figs. 2 and 4). For example, on 18 March, 2009, the VFR was 60 %. In order to better understand the

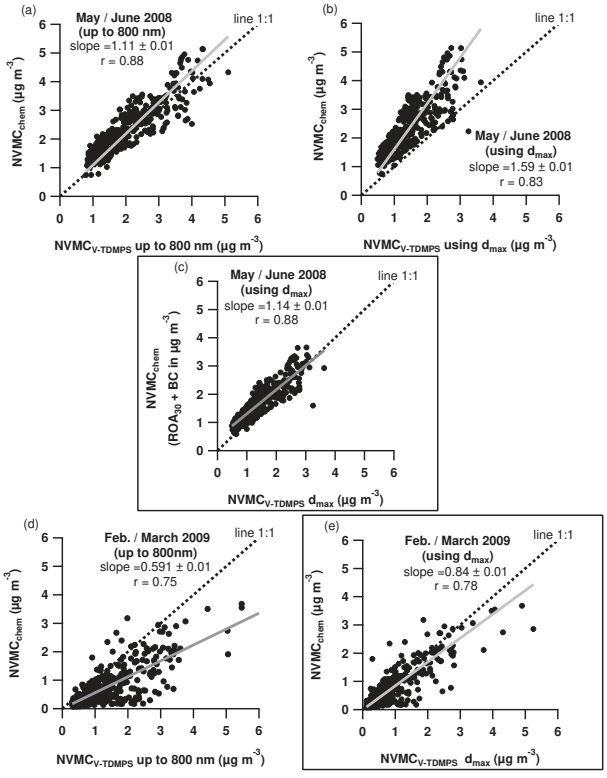

Figure 5. Comparison of the estimated ($NVMC_{est}$) with the measured ($NVMC_{meas}$) non-volatile particle mass concentration (NVMC). Three different approaches were used to estimate the non-volatile particle mass fraction; using the full V-TDMPS size range, (up to 800 nm) or a time-dependent upper size cutting (d_{max}) and finally for May–June 2008, the non-volatile organic aerosol (NVOA) was also estimated based on only 30 % of the measured LV-OOA ($NVOA_{30}$). The two encased scatterplots correspond to the better solution obtained for each periods (see text for discussion).

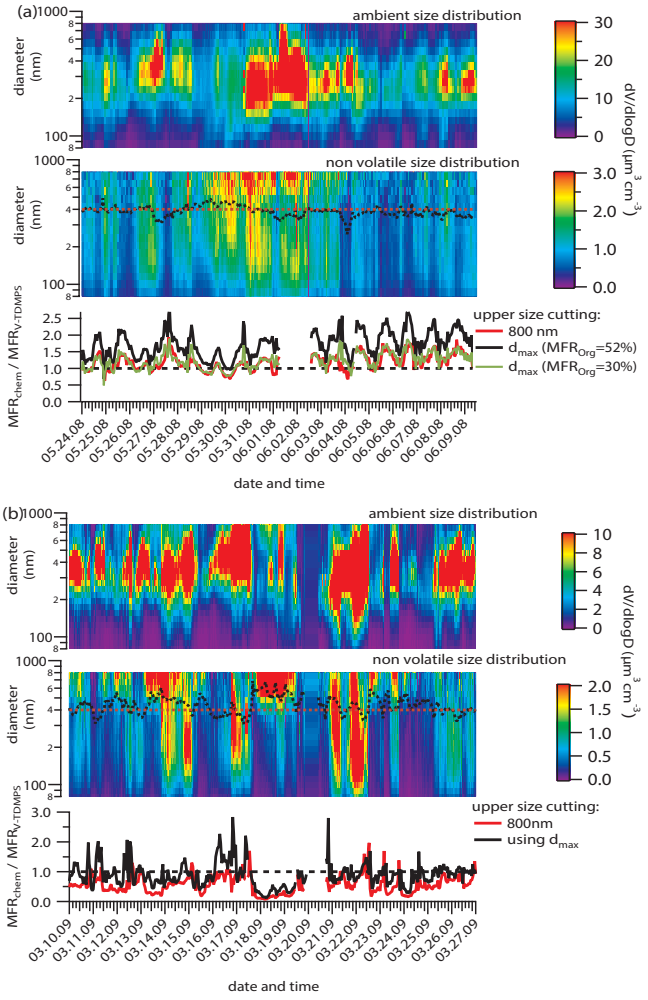

Figure 6. Cross-sensitivity effects of the sea-spray source: Particle volume–size distributions upstream and downstream of the thermodenuder, and the ratios of the mass fraction remaining (MFR) estimated to measure at the 2 upper size cutting (800 nm and d_{max}) for **(a)** May–June 2008 and **(b)** February–March 2009. The black and red dotted lines mark the cut-off estimated using d_{max} approach and the mean d_{max} value, respectively (see Sect. 3.4.1).

limits of our approach and to draw some hypotheses to explain the discrepancies, it is essential to go into more details on the different factors that could influence each time period.

3.4 Discussion

Our results suggest that the non-volatile particle mass fraction (NVMF) could be fully explained by BC and non-volatile OA during May–June 2008, while about one third of this balance remained unexplained in February–March 2009. We now scrutinize two reasons for this deviation: particle-size distribution and chemical particle composition.

3.4.1 Influence of the super micrometer particles

Figure 6 shows contour diagrams of the ambient and non-volatile particle volume–size distributions, and the ratios between AMS/MAAP-based and TDMPS-based non-volatile particle mass concentrations. The basic effect is that the overall particulate volume decreases, and the particle diameters shrink after passage through the TD. This is consistent with earlier observations (Birmili et al., 2010; Ehn et al., 2007; Engler et al., 2007). However, for certain periods, the non-volatile volume size distribution increases in concentration above 400 nm. This effect is visible in Fig. 6, and even better in Fig. 7. Non-volatile particles mostly bigger than 400 nm, can occasionally dominate non-volatile volume size distribution, during events that occurred more frequent in February–March 2009 than in May–June 2008. Prominent examples are 13 and 18 March, 2009.

The non-volatile particles bigger than 400 nm might results either from a drastic change in external particle mixture with particles between 400 and 800 nm containing a significantly higher fraction of entirely non-volatile particles, or to the shrinking of partially volatile particles with initial

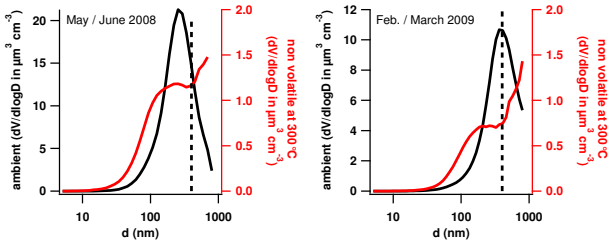

Figure 7. Average particle volume–size distribution measured at ambient temperature (black) and after crossing the TD (red) for the 2 campaigns. The dotted lines mark the mean cut-off diameter of d_{max}.

diameters bigger than 800 nm into the size range measurable by the V-TDMPS instrument. Presence of such particles was related to a few episodes identified as corresponding to marine air masses (Fig. S4 in the Supplement). Comparing the 5-stages Berner impactor samples performed for these specific days to the ones obtained during other air masses influence (Fig. S5 in the Supplement) emphasize the presence of a large coarse mode fraction during marine air masses (Fig. S5 in the Supplement). It is therefore our conclusion that the high value of measured NVMC can be influenced by marine super-µm particles which shrink during passage through the TD and move into the sub-µm measurement range of the TDMPS. In some sense, this is a measurement artifact because these particles can only be detected by the TDMPS downstream of the thermodenuder, not upstream. However, in absence of direct measurement of the mixing state of the particle, we cannot completely exclude a minor influence of the mixing state of the particles.

It was a conspicuous observation that the events on 13 and 18 March, 2009, were connected with maritime air masses, as indicated by 96 h back trajectories from the NOAA HYSPLIT trajectory model (Draxler and Hess, 2004). For example, on 18 March 2009, the air mass originated over the Atlantic, spending only the last 15–16 h over the continent before reaching Melpitz (Fig. S4 in the Supplement). By crossing polluted areas, the marine aerosol aged quickly either by mixing and/or condensation with other aerosols or by heterogeneous reactions (e.g., conversion of NaCl into $NaNO_3$ and/or Na_2SO_4) as well as by in-cloud processes. Therefore, the air mass reaching Melpitz needs to be considered as processed marine air mass rather than fresh marine air mass. Analyses of 5-stages Berner impactor samples for this day revealed unusually high contributions of sulfate, nitrate, chloride, and sodium in the coarse mode (stage 4), which are indicators of sea spray origin particles (Fig. S5 in the Supplement).

Similar events took place on 13 March 2009, compared to 11 March 2009, which was under stronger continental influence (Fig. S4 in the Supplement). The nitrate mass concentration on stage 4 has to be related to the presence of sodium nitrate, a result of the reaction of NaCl and HNO_3 (e.g., Dasgupta et al., 2007). Contrary to ammonium nitrate, which is a semi-volatile compound, sodium nitrate is a low-volatile compound (volatilization temperature > 300 °C, Pinnick et al., 1987), considered to represent a permanent removal pathway for atmospheric nitrate. A similar mechanism can also lead to the formation of sodium sulfate (e.g., Sievering et al., 1995). A similar conclusion can be drawn for sulfate salts.

Moreover, it is known that organic acids can contribute to the chloride depletion on marine aerosol, leading to the formation of sodium salts (e.g., Kerminen et al., 1999; Zhao and Gao, 2008). Consequently, an interesting parallel can be drawn to volatility measurements of succinic acid and its disodium salts made by Wu et al. (2009). Although succinic acid is a semi-volatile compound that fully evaporates at 65 °C, in similar sampling conditions than the present study, Wu et al. (2009) demonstrated that its disodium salt shows a mass fraction remaining of 40 % after being heated at 300 °C. Consequently, regarding the strong marine air mass influence, the presence of such compounds in the coarse mode and after crossing the TD is highly possible and should strongly influence the non-volatile organic mass fractions. Although a strong influence of the super-µm particles on the V-TDMPS measurements was clearly identify, it is not possible to provide a clear picture of the chemical composition of this non-volatile fraction, and to confirm or reject the presence of sodium salts in the resulting super-µm non-volatile fraction. This is because no direct measurements of either super-µm particles or the aerosol chemical composition downstream of the TD were performed. The previous discussion based on laboratory volatility measurements and literature values indicates that the volatility of the marine particles can largely differ from those of continental origin.

Since this artifact is strongly depending on the ambient super-µm particles concentration, a time-dependent estimation of this contribution has to be made. Therefore, estimation of the upper size range of the TD measurements was made derived from the approach proposed by Stanier et al. (2004) for hygroscopicity measurements (Eq. 2).

$$d_{max} = d_{800} \times \sqrt[3]{VFR_{800}}, \quad (2)$$

where d_{max} represents the upper size range considered for the V-TDMPS measurements; $d_{800} = 800$ nm (the upper size range of the ambient TDMPS); and VFR_{800} is the volume fraction remaining calculated using the entire V-TDMPS size range previously described. The time series of the d_{max} value of each campaign is included in Fig. 6. A mean upper size range of 385 ± 40 nm and 441 ± 77 nm was found for the summer and winter campaigns, respectively, in agreement with our estimation of an upper size cutting of 400 nm. According to that, the NVMC was recalculated using the obtained time-dependent upper size range (Figs 3–6). The corrected results reveal that on average the VFR is still under the uncertainties of values obtained using the entire V-TDMPS size range ($VFR_{(d_{max})} = 8 \pm 2$ % and 12 ± 7 % for 2008 and

2009, respectively). This indicates that during some specific periods, the upper size range of the V-TDMPS plays an important role in the estimation of the VFR. This is confirming our hypothesis that during such a period, the presence of an artifact coming from shrinking of the super-µm particles to sub-µm size range when crossing the TD must be considered.

A direct consequence is the enhancement of the BC contribution of total non-volatile mass concentration for 2008 and 2009, respectively (Fig. 3b, d) and the non-volatile mass concentration for February–March 2009 can be explained by the model with still an underestimation of around 14 % which might be related to contribution of non-detected compounds (Figs. 4 and 5e). Based on the reconstructed non-volatile mass, it suggests that non-volatile aerosol at 300 °C was made, on averaged, for 59 ± 6 % of BC and 41 ± 13 % of non-volatile OA during this period. However, the reconstructed non-volatile mass fraction for May–June 2008 strongly over-estimates the measured one (Fig. 5b). This might be interpreted as an overestimation of the non-volatile OA mass concentration (Fig. S2b in the Supplement) resulting on change of the thermodynamic properties of the summer LV-OOA compared to the winter LV-OOA. Nevertheless, no significant change on the correlation coefficient (r) was observed for this period, indicating that only the absolute non-volatile mass concentration was affected by the adjustment of the upper size range and not the time series itself in opposite contrast to the February–March 2009 campaign. Consequently, larger particles seem to have a lower influence in this period than during February–March 2009.

3.4.2 Influence of the chemical composition

Estimation of the non-volatile aerosol mass was only based on the chemical composition measured by the AMS, and the BC concentration, measured by the MAAP. Therefore, the presence of non-detected compounds like crustal material and/or sea salts has to be considered. The contribution of non-considered water soluble inorganic ions (e.g., other water soluble ions like Ca^{2+}, Na^{+}, Mg^{2+} and K^{+}) represents, on averaged, 1.8 % of the measured $PM_{2.5}$ mass concentration in May–June 2008 and 2.5 % of the measured PM_1 mass in February–March 2009. Additionally, identified species of daily PM_1 filter explain on average 82 ± 12 % of the total filter mass in February–March 2009. Consequently, it is reasonable to consider that chemical particle composition was usually fully explained and that, finally, the non-considered compounds might have a small influence on the reconstruction of the non-volatile fraction. However, as mentioned earlier for the ambient mass closure, uncertainties on the MAAP and AMS measurements as well as on the estimation of the NVMC have also to be considered here too.

The estimation of the non-volatile OA concentration was based on the assumption that the LV-OOA's mass fraction remaining is constant over time and using the volatility properties of the HULIS surrogate. In May–June 2008, estimated non-volatile mass fraction is slightly overestimated during daytime (especially in the afternoon), while during nighttime; the model underestimated the non-volatile mass fraction (Fig. 4). It is known that the organic's oxidation state and/or particles' aging change during daytime (Poulain et al., 2011); therefore, it might directly affect the volatility properties of the OA. Consequently, differences in the volatility properties of the two LV-OOA factors may result from the differences in their oxidation states. To check this hypothesis, mass spectra differences were highlighted and plotted in Fig. 8, f44 (the fraction of m/z 44 to total organic mass spectra) vs. f43 (the fraction of m/z 43 to total organic mass spectra) in the triangular space presented by Ng et al. (2010). This triangle plot represents a simple and practical approach to compare different organic factors with different oxidation levels since they will fall in different areas of the triangle. The less oxidized factors (e.g., HOA) are usually present in the bottom of the triangle, whereas the most oxidized factors (e.g., LV-OOA) are usually present in the upper part of the triangle. The top part of the triangle tend to suggest that SOA oxidation level become more and more similar after long aging processes (Ng et al., 2010). Comparing the position of each LV-OOA factor highlights that winter LV-OOA was located slightly above the summer LV-OOA, indicating that winter LV-OAA was more oxygenated than the one in summer. This small difference in term of oxidation state might explain the observed change in the volatility properties of the two LV-OOA factors and the fact that the less volatile factor (winter time, MFR 52 %) is also the one with the highest oxidation level.

Another possible indication on the change of OA volatility is the comparison between the full V-TDMPS size range and the corrected one using d_{max} (Fig. 5a, b). As previously mentioned, in February–March 2009, the time series of the non-volatile mass concentration was strongly affected by the V-TDMPS resizing, while only a scale down of the mass concentration was observed in May–June 2008. Decreasing the upper size range of the V-TDMPS only influence the correlation slope for the 2008 campaign while the correlation coefficient remains nearly constant (Fig. 5a, b). This can also be interpreted as an overestimation of the non-volatile OA mass concentration. Therefore, change of the organic aerosol volatility was investigated by increasing the organic aerosol volatility. Assuming a MFR of 30 % for the LV-OOA ($NVOA_{30}$), the lowest value reported by Huffman et al. (2009), instead of 52 %, strongly improves the comparison with the measured non-volatile mass using a time-dependent upper size cutting (d_{max}) (slope 1.14 and $r = 0.88$, Fig. 5c). $NVOA_{30}$ mass concentration also better correlates with the non-volatile mass than before (Fig. S4c in the Supplement). As previously mentioned, BC concentration depends on the value of the mass coefficient absorption. Increasing this parameter by 20 % (i.e., using the default instrument value) has a small influence on the regression line (+0.1) compared to

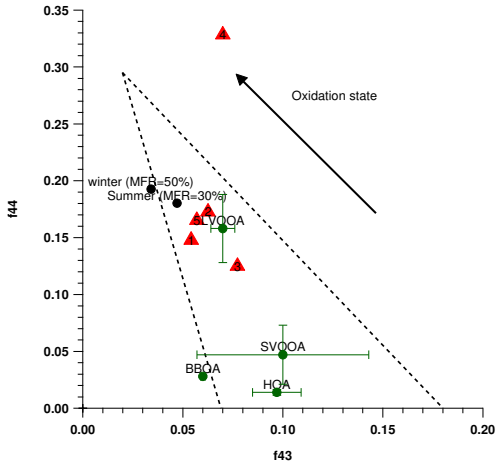

Figure 8. f44 vs. f43 of each LV-OOA factors in the triangle space determined by Ng et al. (2010). The green points referred to the average values (± standard deviation) of factors used by Ng et al. (2010). Red triangle and numbers referred to different examples of LV-OOA factors (1: Hersey et al., 2011, 2: Lanz et al., 2007, 3: Ulbrich et al., 2009, 4: Robinson et al., 2011, 5: Crippa et al., 2013) illustrating the individual variability of LV-OOA.

non-volatile OA. Consequently, change on the MFR of LV-OOA seems to be the dominant factor.

Another source of uncertainty is the appropriate estimation of the non-volatile aerosol density which depends on the chemical composition of the non-volatile aerosol as previously seen for ambient measurements. Here a constant density value of 1.6 g cm^{-3} was used, thus, changes of the density value will influence the present results. Due to the uncertainty of the BC density and the real chemical composition of the non-volatile aerosol, an uncertainty of 10 % can be reasonably expected. Considering the 10 % of the V-TDMPS, a global uncertainty of 20 % for the V-TDMPS mass concentration is estimated. However, the high degree of correlation obtained between the reconstructed and the measured non-volatile mass concentration (Fig. 5c, e) confirmed that BC and non-volatile OA can be used to fully explain the measured non-volatile mass concentration. Subsequently, direct measurements would be necessary to improve the non-volatile OA estimation and to provide exact time-dependency estimations of the non-volatile aerosol mass concentration.

4 Conclusions

Non-volatile particles are measured continuously at the TROPOS Central European research station Melpitz (Germany) by a V-TDMPS instrument consisting of a twin mobility particle sizer and a thermodenuder operating at 300 °C. These measurements are supplemented by a MAAP instrument, from which black carbon (BC) concentrations are derived. During specialized field campaigns in May–June 2008 and February–March 2009, chemical particle composition was determined using an AMS and MAAP. The remaining volume fraction (VFR) was 17 % in 2008 and 11 % in 2009. We estimated the non-volatile particle mass concentration (NVMC) by two methods, based either on the TDMPS particle volume and an assumed constant particle density, or the sum of non-volatile chemical compounds identified in the AMS and the MAAP. Backward air mass trajectories as well as impactor particle mass–size distribution measurements point out that the non-volatile mass fraction measured during the February–March 2009 period was strongly influenced by aged marine particles bigger than 1 µm. Similar influence of the super-µm particles was also observed for May–June 2008. Limiting the TDMPS range to 400 nm allowed limiting the interference of these aged marine particles, yielding a better mass balance for the non-volatile particles. These results highlight the potential cross-sensitivity of partially volatile coarse mode particles on sub-µm volatility measurements, as long as these particles are not removed from the sample, e.g., by a pre-impactor. It might be desirable in the future to extend the V-TDMPS with an aerodynamic particles sizer (APS), or alternatively remove particles by a pre-impactor.

Comparing the two periods, our results suggest a possible change on the LV-OOA volatility with a highest volatility in May–June 2008 (MFR = 30 %) than in February–March 2009 (MFR = 52 %). A possible reason might be a change to oxidation state and/or LV-OOA origins. Nevertheless, our results emphasize a significant contribution of OA to the non-volatile particle mass fraction (53 % and 41 % in May–June 2008 and February–March 2009, respectively) and also suggest a possible change of their volatility properties during the run of a year. Since contribution of undetected and non-volatile compounds (e.g., dust, other inorganic ions) cannot be completely excluded, the present NVOA values have to be considered as the upper limit that may be expected for each period. Therefore direct measurements using aerosol mass spectrometer downstream of the thermodenuder are needed (for example with AMS during intensive period or with ToF-ACSM for longer period). Nevertheless, our results clearly indicate that 300 °C non-volatile organic matter might represent an important part of the non-volatile fraction of the atmospheric particles investigated in this work. Considering the limitation of our approach (i.e., proper mass balance closure of the ambient PM_1 and a minor contribution of dust and sea salt to the total PM_1 mass), our findings could be used to extrapolate the maximum expected non-volatile organic mass concentration from similar setup measurements such as for the long-term measurements at Melpitz and within the GUAN network. Because OA do not completely evaporate at 300 °C, the non-volatile OA particle mass fraction would remain in the particle phase.

Appendix A: Verification of thermodenuder efficiency

To verify the efficiency of our thermodenuder (Wehner type TD) as a function of residence time, we conducted a sensitivity experiment. For this purpose, two technically identical mobility particle size spectrometers were set up at the research station Leipzig-TROPOS (Germany), each equipped with identical thermodenuders upstream of the device (Fig. A1). The temperature in both thermodenuders was set to 300 °C, as during the long-term measurements in Melpitz. Thermodenuder 1 was flushed by a constant flow of $Q_1 = 3\,\mathrm{L\,min^{-1}}$, which also corresponds to the nominal sampling flow during long-term measurements. Thermodenuder 2 was operated in the same fashion except that its sampling flow Q_2 could be varied between 1 and $10\,\mathrm{L\,min^{-1}}$ by means of an additional make-up flow. During the experiment, approximately 16 days of valid data were collected. Four different settings for Q_2 were employed: 1, 3, 5, and $10\,\mathrm{L\,min^{-1}}$. Due to the pseudo isokinetic split between SMPS and make-up flow, a slight uncertainty on the SMPS might be expected. Quality check of the two mobility particle size spectrometers was performed by measuring non-heated ambient particles for each value of Q_2 (these periods correspond to the gaps in Fig. A2). The agreement between the two instruments is in line with the instrumental uncertainties reported by Wiedensohler et al. (2012).

The results of the experiment with ambient aerosols are depicted in Fig. A2. The upper graph shows the time series of the remaining particulate volume (< 800 nm) of both instruments (V_1 and V_2). It can be seen that V_1 and V_2 follow each other very closely over most parts of the experiment, including large overall variations of total particle volume. The bottom graph of Fig. A2 confirms that the ratio V_2 / V_1 between the volumes remaining downstream of the thermodenuders straddles around the value of 1.

Table A1. Ratio V_2 / V_1 between the remaining volumes as a function of the sampling flow through thermodenuder 2. The minimum residence time T_{res} of the air sample in the heating unit is indicated in s.

Q_2 ($\mathrm{L\,min^{-1}}$)	T_{res} (in s)	Volume ratio (V_2 / V_1)		
		Mean	SD.	Median
1	9.4	1.03	0.13	1.02
3	3.1	1.00	0.09	0.99
5	1.9	1.00	0.12	0.99
10	0.9	1.05	0.08	1.06

Figure A3 and Table A1 sort the data into different values of Q_2. For the nominal flow $Q_1 = Q_2 = 3\,\mathrm{L\,min^{-1}}$ the thermodenuders agree very well on average (V_2 / $V_1 = 1.00$). The same holds for $Q_2 = 5\,\mathrm{L\,min^{-1}}$. Increasing the residence time by choosing $Q_2 = 1\,\mathrm{L\,min^{-1}}$ yields V_2 / $V_1 =$ 1.03, i.e., a slight decrease in the efficiency of thermodenuder 2, despite an increased residence time. For $Q_2 = 10\,\mathrm{L\,min^{-1}}$, i.e., the shortest residence time, V_2 / $V_1 = 1.05$. The latter value might be interpreted as a decrease in thermodenuder efficiency as a result of decreasing residence time. It needs to be noted, however, that these deviations are on the order of the measurement accuracy of the instruments.

Our conclusion is we cannot observe any remarkable dependency of the remaining volume after the thermodenuder on the sampling flow. We can safely assume this across the flow range $1\,\mathrm{L\,min^{-1}} < Q_2 < 5\,\mathrm{L\,min^{-1}}$, where $Q_2 = 10\,\mathrm{L\,min^{-1}}$ There is therefore no indication that the residence in the thermodenuder (3.1 s at $Q = 3\,\mathrm{L\,min^{-1}}$) would be insufficient to evaporate all particulate material volatile at 300 °C.

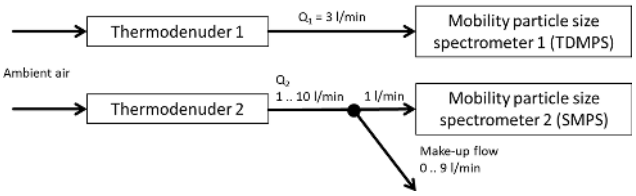

Figure A1. Experimental setup to test the sensitivity of the thermodenuder efficiency as a function of residence time.

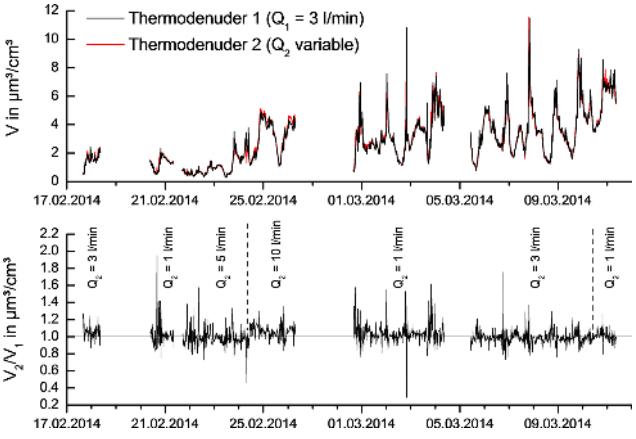

Figure A2. Upper graph: time series of particulate volume (< 800 nm) of ambient aerosol remaining after passage through the thermodenuders at 300 °C. Bottom graph: ratio V_2 / V_1 between the volumes remaining downstream of the thermodenuders.

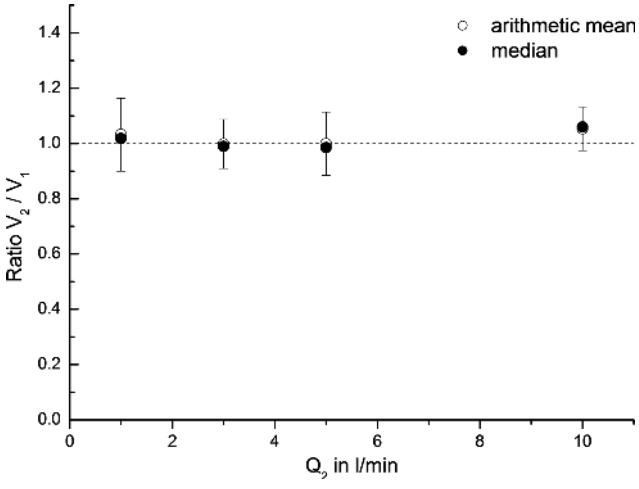

Figure A3. Ratio V_2 / V_1 between the remaining volumes as a function of the sampling flow through thermodenuder 2. Error bars correspond to standard deviation.

The Supplement related to this article is available online at doi:10.5194/acp-14-10145-2014-supplement.

Acknowledgements. We gratefully acknowledge support by the German Federal Environment Agency (Umweltbundesamt), grants no. 351 03 031 and 351 01 038, and UFOPLAN grant 3703 43 200 (title *Erfassung der Zahl feiner und ultrafeiner Partikel in der Außenluft*). We acknowledge support by the European Integrated Project on Aerosol Cloud Climate and Air Quality Interaction (EUCAARI). We further appreciate extensive instrumental support by Joachim Grüner and Thomas Tuch at the TROPOS Melpitz field site.

Edited by: V.-M. Kerminen

References

Aas, W., Tsyro, S., Bieber, E., Bergström, R., Ceburnis, D., Ellermann, T., Fagerli, H., Frölich, M., Gehrig, R., Makkonen, U., Nemitz, E., Otjes, R., Perez, N., Perrino, C., Prévôt, A. S. H., Putaud, J.-P., Simpson, D., Spindler, G., Vana, M., and Yttri, K. E.: Lessons learnt from the first EMEP intensive measurement periods, Atmos. Chem. Phys., 12, 8073–8094, doi:10.5194/acp-12-8073-2012, 2012.

An, W. J., Pathak, R. K., Lee, B. H., and Pandis, S. N.: Aerosol volatility measurement using an improved thermodenuder: Application to secondary organic aerosol, J. Aerosol Sci., 38, 305–314, doi:10.1016/j.jaerosci.2006.12.002, 2007.

Attfield, M. D., Schleiff, P. L., Lubin, J. H., Blair, A., Stewart, P. A., Vermeulen, R., Coble, J. B., and Silverman, D. T.: The Diesel Exhaust in Miners Study: A Cohort Mortality Study With Emphasis on Lung Cancer, Journal of the Natl. Cancer I., 104, 869–883, doi:10.1093/Jnci/Djs035, 2012.

Bahreini, R., Ervens, B., Middlebrook, A. M., Warneke, C., de Gouw, J. A., DeCarlo, P. F., Jimenez, J. L., Brock, C. A., Neuman, J. A., Ryerson, T. B., Stark, H., Atlas, E., Brioude, J., Fried, A., Holloway, J. S., Peischl, J., Richter, D., Walega, J., Weibring, P., Wollny, A. G., and Fehsenfeld, F. C.: Organic aerosol formation in urban and industrial plumes near Houston and Dallas, Texas, J. Geophys. Res., 114, D00f16, doi:10.1029/2008jd011493, 2009.

Berner, A. and Lurzer, C.: Mass Size Distributions of Traffic Aerosols at Vienna, J. Phys. Chem., 84, 2079–2083, doi:10.1021/j100453a016, 1980.

Birmili, W., Stratmann, F., and Wiedensohler, A.: Design of a DMA-based size spectrometer for a large particle size range and stable operation, J. Aerosol Sci., 30, 549–553, doi:10.1016/S0021-8502(98)00047-0, 1999.

Birmili, W., Schepanski, K., Ansmann, A., Spindler, G., Tegen, I., Wehner, B., Nowak, A., Reimer, E., Mattis, I., Müller, K., Brüggemann, E., Gnauk, T., Herrmann, H., Wiedensohler, A., Althausen, D., Schladitz, A., Tuch, T., and Löschau, G.: A case of extreme particulate matter concentrations over Central Europe caused by dust emitted over the southern Ukraine, Atmos. Chem. Phys., 8, 997–1016, doi:10.5194/acp-8-997-2008, 2008.

Birmili, W., Weinhold, K., Nordmann, S., Wiedensohler, A., Spindler, G., Müller, K., Herrmann, H., Gnauk, T., Pitz, M., Cyrys, J., Flentje, H., Nickel, C., Kuhlbusch, T. A. J., and Löschau, G.: Atmospheric aerosol measurements in the German Ultrafine Aerosol Network (GUAN): Part 1 – soot and particle number size distribution, Gefahrst. Reinh. Luft., 69, 137–145, 2009.

Birmili, W., Heinke, K., Pitz, M., Matschullat, J., Wiedensohler, A., Cyrys, J., Wichmann, H.-E., and Peters, A.: Particle number size distributions in urban air before and after volatilisation, Atmos. Chem. Phys., 10, 4643–4660, doi:10.5194/acp-10-4643-2010, 2010.

Bohlmann, N., Meissner, R., Bernsdorf, S., Bohme, F., Russow, R., and Wegener, U.: Studies of atmospheric nitrogen deposition in a mire of the German National Park Hochharz Mountains using two different methods, Water Air Soil Poll., 168, 17–32, doi:10.1007/s11270-005-0587-0, 2005.

Bond, T. C. and Bergstrom, R. W.: Light absorption by carbonaceous particles: An investigative review, Aerosol Sci. Technol., 40, 27–67, doi:10.1080/02786820500421521, 2006.

Burtscher, H., Baltensperger, U., Bukowiecki, N., Cohn, P., Hüglin, C., Mohr, M., Matter, U., Nyeki, S., Schmatloch, V., Streit, N., and Weingartner, E.: Separation of volatile and non-volatile aerosol fractions by thermodesorption: instrumental development and applications, J. Aerosol Sci., 32, 427–442, doi:10.1016/S0021-8502(00)00089-6, 2001.

Canagaratna, M. R., Jayne, J. T., Jimenez, J. L., Allan, J. D., Alfarra, M. R., Zhang, Q., Onasch, T. B., Drewnick, F., Coe, H., Middlebrook, A., Delia, A., Williams, L. R., Trimborn, A. M., Northway, M. J., Decarlo, P. F., Kolb, C. E., Davidovits, P., and Worsnop, D. R.: Chemical and microphysical characterization of ambient aerosols with the Aerodyne aerosol mass spectrometer, Mass Spectrom. Rev., 26, 185–222, doi:10.1002/mas.20115, 2007.

Canonaco, F., Crippa, M., Slowik, J. G., Baltensperger, U., and Prévôt, A. S. H.: SoFi, an IGOR-based interface for the efficient use of the generalized multilinear engine (ME-2) for the source apportionment: ME-2 application to aerosol mass spectrometer data, Atmos. Meas. Tech., 6, 3649–3661, doi:10.5194/amt-6-3649-2013, 2013.

Cheng, Y. F., Berghof, M., Garland, R. M., Wiedensohler, A., Wehner, B., Muller, T., Su, H., Zhang, Y. H., Achtert, P., Nowak, A., Poschl, U., Zhu, T., Hu, M., and Zeng, L. M.: Influence of soot mixing state on aerosol light absorption and single scattering albedo during air mass aging at a polluted regional site in northeastern China, J. Geophys. Res., 114, D00G10, doi:10.1029/2008jd010883, 2009.

Crippa, M., DeCarlo, P. F., Slowik, J. G., Mohr, C., Heringa, M. F., Chirico, R., Poulain, L., Freutel, F., Sciare, J., Cozic, J., Di Marco, C. F., Elsasser, M., Nicolas, J. B., Marchand, N., Abidi, E., Wiedensohler, A., Drewnick, F., Schneider, J., Borrmann, S., Nemitz, E., Zimmermann, R., Jaffrezo, J.-L., Prévôt, A. S. H., and Baltensperger, U.: Wintertime aerosol chemical composition and source apportionment of the organic fraction in the metropolitan area of Paris, Atmos. Chem. Phys., 13, 961–981, doi:10.5194/acp-13-961-2013, 2013.

Crippa, M., Canonaco, F., Lanz, V. A., Äijälä, M., Allan, J. D., Carbone, S., Capes, G., Ceburnis, D., Dall'Osto, M., Day, D. A., DeCarlo, P. F., Ehn, M., Eriksson, A., Freney, E., Hildebrandt Ruiz,

L., Hillamo, R., Jimenez, J. L., Junninen, H., Kiendler-Scharr, A., Kortelainen, A.-M., Kulmala, M., Laaksonen, A., Mensah, A. A., Mohr, C., Nemitz, E., O'Dowd, C., Ovadnevaite, J., Pandis, S. N., Petäjä, T., Poulain, L., Saarikoski, S., Sellegri, K., Swietlicki, E., Tiitta, P., Worsnop, D. R., Baltensperger, U., and Prévôt, A. S. H.: Organic aerosol components derived from 25 AMS data sets across Europe using a consistent ME-2 based source apportionment approach, Atmos. Chem. Phys., 14, 6159–6176, doi:10.5194/acp-14-6159-2014, 2014.

Dasgupta, P. K., Campbell, S. W., Al-Horr, R. S., Ullah, S. M. R., Li, J. Z., Amalfitano, C., and Poor, N. D.: Conversion of sea salt aerosol to $NaNO_3$ and the production of HCl: Analysis of temporal behavior of aerosol chloride/nitrate and gaseous HCl/HNO_3 concentrations with AIM, Atmos. Environ., 41, 4242–4257, doi:10.1016/j.atmosenv.2006.09.054, 2007.

DeCarlo, P. F., Kimmel, J. R., Trimborn, A., Northway, M. J., Jayne, J. T., Aiken, A. C., Gonin, M., Fuhrer, K., Horvath, T., Docherty, K. S., Worsnop, D. R., and Jimenez, J. L.: Field-deployable, high-resolution, time-of-flight aerosol mass spectrometer, Anal. Chem., 78, 8281–8289, doi:10.1021/ac061249n, 2006.

Donahue, N. M., Robinson, A. L., Stanier, C. O., and Pandis, S. N.: Coupled partitioning, dilution, and chemical aging of semivolatile organics, Environ. Sci. Technol., 40, 2635–2643, doi:10.1021/Es052297c, 2006.

Donahue, N. M., Epstein, S. A., Pandis, S. N., and Robinson, A. L.: A two-dimensional volatility basis set: 1. organic-aerosol mixing thermodynamics, Atmos. Chem. Phys., 11, 3303–3318, doi:10.5194/acp-11-3303-2011, 2011.

Donahue, N. M., Henry, K. M., Mentel, T. F., Kiendler-Scharr, A., Spindler, C., Bohn, B., Brauers, T., Dorn, H. P., Fuchs, H., Tillmann, R., Wahner, A., Saathoff, H., Naumann, K. H., Mohler, O., Leisner, T., Muller, L., Reinnig, M. C., Hoffmann, T., Salo, K., Hallquist, M., Frosch, M., Bilde, M., Tritscher, T., Barmet, P., Praplan, A. P., DeCarlo, P. F., Dommen, J., Prevot, A. S. H., and Baltensperger, U.: Aging of biogenic secondary organic aerosol via gas-phase OH radical reactions, P. Natl. Acad. Sci., 109, 13503–13508, doi:10.1073/pnas.1115186109, 2012a.

Donahue, N. M., Kroll, J. H., Pandis, S. N., and Robinson, A. L.: A two-dimensional volatility basis set – Part 2: Diagnostics of organic-aerosol evolution, Atmos. Chem. Phys., 12, 615–634, doi:10.5194/acp-12-615-2012, 2012b.

Draxler, R. and Hess, G.: Description of the HYSPLIT4 modeling system, NOAA Technical Memorandum, ERL, ARL-224, 2004.

Ehn, M., Petäjä, T., Birmili, W., Junninen, H., Aalto, P., and Kulmala, M.: Non-volatile residuals of newly formed atmospheric particles in the boreal forest, Atmos. Chem. Phys., 7, 677–684, doi:10.5194/acp-7-677-2007, 2007.

Engler, C., Rose, D., Wehner, B., Wiedensohler, A., Brüggemann, E., Gnauk, T., Spindler, G., Tuch, T., and Birmili, W.: Size distributions of non-volatile particle residuals ($D_p < 800$ nm) at a rural site in Germany and relation to air mass origin, Atmos. Chem. Phys., 7, 5785–5802, doi:10.5194/acp-7-5785-2007, 2007.

Faulhaber, A. E., Thomas, B. M., Jimenez, J. L., Jayne, J. T., Worsnop, D. R., and Ziemann, P. J.: Characterization of a thermodenuder-particle beam mass spectrometer system for the study of organic aerosol volatility and composition, Atmos. Meas. Tech., 2, 15–31, doi:10.5194/amt-2-15-2009, 2009.

Freutel, F., Schneider, J., Drewnick, F., von der Weiden-Reinmüller, S.-L., Crippa, M., Prévôt, A. S. H., Baltensperger, U., Poulain, L., Wiedensohler, A., Sciare, J., Sarda-Estève, R., Burkhart, J. F., Eckhardt, S., Stohl, A., Gros, V., Colomb, A., Michoud, V., Doussin, J. F., Borbon, A., Haeffelin, M., Morille, Y., Beekmann, M., and Borrmann, S.: Aerosol particle measurements at three stationary sites in the megacity of Paris during summer 2009: meteorology and air mass origin dominate aerosol particle composition and size distribution, Atmos. Chem. Phys., 13, 933–959, doi:10.5194/acp-13-933-2013, 2013.

Fuller, K. A., Malm, W. C., and Kreidenweis, S. M.: Effects of mixing on extinction by carbonaceous particles, J. Geophys. Res., 104, 15941–15954, doi:10.1029/1998jd100069, 1999.

Gurjar, B. R., Jain, A., Sharma, A., Agarwal, A., Gupta, A., Nagpure, A. S., and Lelieveld, J.: Human health risks in megacities due to air pollution, Atmos. Environ., 44, 4606–4613, doi:10.1016/j.atmosenv.2010.08.011, 2010.

Hallquist, M., Wenger, J. C., Baltensperger, U., Rudich, Y., Simpson, D., Claeys, M., Dommen, J., Donahue, N. M., George, C., Goldstein, A. H., Hamilton, J. F., Herrmann, H., Hoffmann, T., Iinuma, Y., Jang, M., Jenkin, M. E., Jimenez, J. L., Kiendler-Scharr, A., Maenhaut, W., McFiggans, G., Mentel, Th. F., Monod, A., Prévôt, A. S. H., Seinfeld, J. H., Surratt, J. D., Szmigielski, R., and Wildt, J.: The formation, properties and impact of secondary organic aerosol: current and emerging issues, Atmos. Chem. Phys., 9, 5155–5236, doi:10.5194/acp-9-5155-2009, 2009.

Hersey, S. P., Craven, J. S., Schilling, K. A., Metcalf, A. R., Sorooshian, A., Chan, M. N., Flagan, R. C., and Seinfeld, J. H.: The Pasadena Aerosol Characterization Observatory (PACO): chemical and physical analysis of the Western Los Angeles basin aerosol, Atmos. Chem. Phys., 11, 7417–7443, doi:10.5194/acp-11-7417-2011, 2011.

Huffman, J. A., Ziemann, P. J., Jayne, J. T., Worsnop, D. R., and Jimenez, J. L.: Development and characterization of a fast-stepping/scanning thermodenuder for chemically-resolved aerosol volatility measurements, Aerosol Sci. Technol., 42, 395–407, doi:10.1080/02786820802104981, 2008.

Huffman, J. A., Docherty, K. S., Aiken, A. C., Cubison, M. J., Ulbrich, I. M., DeCarlo, P. F., Sueper, D., Jayne, J. T., Worsnop, D. R., Ziemann, P. J., and Jimenez, J. L.: Chemically-resolved aerosol volatility measurements from two megacity field studies, Atmos. Chem. Phys., 9, 7161–7182, doi:10.5194/acp-9-7161-2009, 2009.

IPCC: Climate Change 2007: The physical science basis, edited by: Solomon, S., Qin, D., Manning, M., Chen, Z., Marquis, M., Averyt, K. B., Tignor, M., and Miller, H. L., Cambridge University Press, Cambridge, 2007.

Janssen, N. A., Gerlofs-Nijland, M. E., Lanki, T., Salonen, R. O., Cassee, F., Hoek, G., Fischer, P., Brunekreef, B., and Krzyzanowski, M.: Health effects of black carbon, World Health Organization Regional Office for Europe, Copenhagen, Denmark, 2012.

Jickells, T. D., An, Z. S., Andersen, K. K., Baker, A. R., Bergametti, G., Brooks, N., Cao, J. J., Boyd, P. W., Duce, R. A., Hunter, K. A., Kawahata, H., Kubilay, N., laRoche, J., Liss, P. S., Mahowald, N., Prospero, J. M., Ridgwell, A. J., Tegen, I., and Torres, R.: Global iron connections between desert dust, ocean biogeochemistry, and climate, Science, 308, 67–71, doi:10.1126/science.1105959, 2005.

Jimenez, J. L., Canagaratna, M. R., Donahue, N. M., Prevot, A. S. H., Zhang, Q., Kroll, J. H., DeCarlo, P. F., Allan, J. D., Coe, H., Ng, N. L., Aiken, A. C., Docherty, K. S., Ulbrich, I. M., Grieshop, A. P., Robinson, A. L., Duplissy, J., Smith, J. D., Wilson, K. R., Lanz, V. A., Hueglin, C., Sun, Y. L., Tian, J., Laaksonen, A., Raatikainen, T., Rautiainen, J., Vaattovaara, P., Ehn, M., Kulmala, M., Tomlinson, J. M., Collins, D. R., Cubison, M. J., E, Dunlea, J., Huffman, J. A., Onasch, T. B., Alfarra, M. R., Williams, P. I., Bower, K., Kondo, Y., Schneider, J., Drewnick, F., Borrmann, S., Weimer, S., Demerjian, K., Salcedo, D., Cottrell, L., Griffin, R., Takami, A., Miyoshi, T., Hatakeyama, S., Shimono, A., Sun, J. Y., Zhang, Y. M., Dzepina, K., Kimmel, J. R., Sueper, D., Jayne, J. T., Herndon, S. C., Trimborn, A. M., Williams, L. R., Wood, E. C., Middlebrook, A. M., Kolb, C. E., Baltensperger, U., and Worsnop, D. R.: Evolution of organic aerosols in the atmosphere, Science, 326, 1525–1529, doi:10.1126/science.1180353, 2009.

Kanakidou, M., Seinfeld, J. H., Pandis, S. N., Barnes, I., Dentener, F. J., Facchini, M. C., Van Dingenen, R., Ervens, B., Nenes, A., Nielsen, C. J., Swietlicki, E., Putaud, J. P., Balkanski, Y., Fuzzi, S., Horth, J., Moortgat, G. K., Winterhalter, R., Myhre, C. E. L., Tsigaridis, K., Vignati, E., Stephanou, E. G., and Wilson, J.: Organic aerosol and global climate modelling: a review, Atmos. Chem. Phys., 5, 1053–1123, doi:10.5194/acp-5-1053-2005, 2005.

Kerminen, V. M., Teinila, K., Hillamo, R., and Makela, T.: Size-segregated chemistry of particulate dicarboxylic acids in the Arctic atmosphere, Atmos. Environ., 33, 2089–2100, doi:10.1016/S1352-2310(98)00350-1, 1999.

Koch, D., Schulz, M., Kinne, S., McNaughton, C., Spackman, J. R., Balkanski, Y., Bauer, S., Berntsen, T., Bond, T. C., Boucher, O., Chin, M., Clarke, A., De Luca, N., Dentener, F., Diehl, T., Dubovik, O., Easter, R., Fahey, D. W., Feichter, J., Fillmore, D., Freitag, S., Ghan, S., Ginoux, P., Gong, S., Horowitz, L., Iversen, T., Kirkevåg, A., Klimont, Z., Kondo, Y., Krol, M., Liu, X., Miller, R., Montanaro, V., Moteki, N., Myhre, G., Penner, J. E., Perlwitz, J., Pitari, G., Reddy, S., Sahu, L., Sakamoto, H., Schuster, G., Schwarz, J. P., Seland, Ø., Stier, P., Takegawa, N., Takemura, T., Textor, C., van Aardenne, J. A., and Zhao, Y.: Evaluation of black carbon estimations in global aerosol models, Atmos. Chem. Phys., 9, 9001–9026, doi:10.5194/acp-9-9001-2009, 2009.

Kolb, C. E. and Worsnop, D. R.: Chemistry and Composition of Atmospheric Aerosol Particles, Ann. Rev. Phys. Chem., 63, 471–491, doi:10.1146/annurev-physchem-032511-143706, 2012.

Kondo, Y., Sahu, L., Moteki, N., Khan, F., Takegawa, N., Liu, X., Koike, M., and Miyakawa, T.: Consistency and Traceability of Black Carbon Measurements Made by Laser-Induced Incandescence, Thermal-Optical Transmittance, and Filter-Based Photo-Absorption Techniques, Aerosol Sci. Technol., 45, 295–312, doi:10.1080/02786826.2010.533215, 2011.

Lanz, V. A., Alfarra, M. R., Baltensperger, U., Buchmann, B., Hueglin, C., and Prévôt, A. S. H.: Source apportionment of submicron organic aerosols at an urban site by factor analytical modelling of aerosol mass spectra, Atmos. Chem. Phys., 7, 1503–1522, doi:10.5194/acp-7-1503-2007, 2007.

Lide, D. R.: CRC Handbook of Chemistry and Physics, CRC Press Inc., USA, 1991.

Mazzarella, G., Ferraraccio, F., Prati, M. V., Annunziata, S., Bianco, A., Mezzogiorno, A., Liguori, G., Angelillo, I. F., and Cazzola, M.: Effects of diesel exhaust particles on human lung epithelial cells: An in vitro study, Resp. Med. , 101, 1155–1162, doi:10.1016/j.rmed.2006.11.011, 2007.

Mensah, A. A., Holzinger, R., Otjes, R., Trimborn, A., Mentel, Th. F., ten Brink, H., Henzing, B., and Kiendler-Scharr, A.: Aerosol chemical composition at Cabauw, The Netherlands as observed in two intensive periods in May 2008 and March 2009, Atmos. Chem. Phys., 12, 4723–4742, doi:10.5194/acp-12-4723-2012, 2012.

Molina, M. J. and Molina, L. T.: Megacities and atmospheric pollution, J. Air Waste Manage. Assoc., 54, 644–680, doi:10.1080/10473289.2004.10470936, 2004.

Müller, T., Henzing, J. S., de Leeuw, G., Wiedensohler, A., Alastuey, A., Angelov, H., Bizjak, M., Collaud Coen, M., Engström, J. E., Gruening, C., Hillamo, R., Hoffer, A., Imre, K., Ivanow, P., Jennings, G., Sun, J. Y., Kalivitis, N., Karlsson, H., Komppula, M., Laj, P., Li, S.-M., Lunder, C., Marinoni, A., Martins dos Santos, S., Moerman, M., Nowak, A., Ogren, J. A., Petzold, A., Pichon, J. M., Rodriquez, S., Sharma, S., Sheridan, P. J., Teinilä, K., Tuch, T., Viana, M., Virkkula, A., Weingartner, E., Wilhelm, R., and Wang, Y. Q.: Characterization and intercomparison of aerosol absorption photometers: result of two intercomparison workshops, Atmos. Meas. Tech., 4, 245–268, doi:10.5194/amt-4-245-2011, 2011.

Ng, N. L., Canagaratna, M. R., Zhang, Q., Jimenez, J. L., Tian, J., Ulbrich, I. M., Kroll, J. H., Docherty, K. S., Chhabra, P. S., Bahreini, R., Murphy, S. M., Seinfeld, J. H., Hildebrandt, L., Donahue, N. M., DeCarlo, P. F., Lanz, V. A., Prévôt, A. S. H., Dinar, E., Rudich, Y., and Worsnop, D. R.: Organic aerosol components observed in Northern Hemispheric datasets from Aerosol Mass Spectrometry, Atmos. Chem. Phys., 10, 4625–4641, doi:10.5194/acp-10-4625-2010, 2010.

Nordmann, S., Birmili, W., Weinhold, K., Müller, K., Spindler, G., and Wiedensohler, A.: Measurements of the mass absorption cross section of atmospheric soot particles using Raman spectroscopy, J. Geophys. Res., 118, 12075–12085, doi:10.1002/2013jd020021, 2013.

Ostro, B., Feng, W. Y., Broadwin, R., Green, S., and Lipsett, M.: The effects of components of fine particulate air pollution on mortality in California: Results from CALFINE, Environ. Health Perspect., 115, 13–19, doi:10.1289/Ehp.9281, 2007.

Ovadnevaite, J., Ceburnis, D., Canagaratna, M., berresheim, H., bialek, J., Martucci, G., and Worsnop, D.: On the effect of wind speed on submicron sea salt mass concentrations and source fluxes, J. Geophys. Res., 117, D16201, doi:10.1029/2011JD017379, 2012.

Paatero, P.: The multilinear engine – A table-driven, least squares program for solving multilinear problems, including the *n*-way parallel factor analysis model, J. Comput. Graph. Stat., 8, 854–888, doi:10.2307/1390831, 1999.

Park, K., Kittelson, D. B., Zachariah, M. R., and McMurry, P. H.: Measurement of inherent material density of nanoparticle agglomerates, J. Nanopart. Res., 6, 267–272, doi:10.1023/B:NANO.0000034657.71309.e6, 2004.

Petzold, A. and Schönlinner, M.: Multi-angle absorption photometry – a new method for the measurement of aerosol light absorp-

tion and atmospheric black carbon, J. Aerosol Sci., 35, 421–441, doi:10.1016/j.jaerosci.2003.09.005, 2004.

Philippin, S., Wiedensohler, A., and Stratmann, F.: Measurements of non-volatile fractions of pollution aerosols with an eight-tube volatility tandem differential mobility analyzer (VTDMA-8), J. Aerosol Sci., 35, 185–203, doi:10.1016/j.jaerosci.2003.07.004, 2004.

Pinnick, R. G., Jennings, S. G., and Fernandez, G.: Volatility of Aerosols in the Arid Southwestern United-States, J. Atmos. Sci., 44, 562–576, 1987.

Pope, C. A.: Epidemiology of fine particulate air pollution and human health: Biologic mechanisms and who's at risk?, Environ. Health Perspect., 108, 713–723, 2000.

Pöschl, U.: Atmospheric Aerosols: Composition, Transformation, Climate and Health Effects, Angewandte Chemie International Edition, 44, 7520–7540, doi:10.1002/anie.200501122, 2005.

Pöschl, U., Rudich, Y., and Ammann, M.: Kinetic model framework for aerosol and cloud surface chemistry and gas-particle interactions – Part 1: General equations, parameters, and terminology, Atmos. Chem. Phys., 7, 5989–6023, doi:10.5194/acp-7-5989-2007, 2007.

Poulain, L., Spindler, G., Birmili, W., Plass-Dülmer, C., Wiedensohler, A., and Herrmann, H.: Seasonal and diurnal variations of particulate nitrate and organic matter at the IfT research station Melpitz, Atmos. Chem. Phys., 11, 12579–12599, doi:10.5194/acp-11-12579-2011, 2011.

Robinson, N. H., Hamilton, J. F., Allan, J. D., Langford, B., Oram, D. E., Chen, Q., Docherty, K., Farmer, D. K., Jimenez, J. L., Ward, M. W., Hewitt, C. N., Barley, M. H., Jenkin, M. E., Rickard, A. R., Martin, S. T., McFiggans, G., and Coe, H.: Evidence for a significant proportion of Secondary Organic Aerosol from isoprene above a maritime tropical forest, Atmos. Chem. Phys., 11, 1039–1050, doi:10.5194/acp-11-1039-2011, 2011.

Rose, D., Wehner, B., Ketzel, M., Engler, C., Voigtländer, J., Tuch, T., and Wiedensohler, A.: Atmospheric number size distributions of soot particles and estimation of emission factors, Atmos. Chem. Phys., 6, 1021–1031, doi:10.5194/acp-6-1021-2006, 2006.

Salcedo, D., Onasch, T. B., Dzepina, K., Canagaratna, M. R., Zhang, Q., Huffman, J. A., DeCarlo, P. F., Jayne, J. T., Mortimer, P., Worsnop, D. R., Kolb, C. E., Johnson, K. S., Zuberi, B., Marr, L. C., Volkamer, R., Molina, L. T., Molina, M. J., Cardenas, B., Bernabé, R. M., Márquez, C., Gaffney, J. S., Marley, N. A., Laskin, A., Shutthanandan, V., Xie, Y., Brune, W., Lesher, R., Shirley, T., and Jimenez, J. L.: Characterization of ambient aerosols in Mexico City during the MCMA-2003 campaign with Aerosol Mass Spectrometry: results from the CENICA Supersite, Atmos. Chem. Phys., 6, 925–946, doi:10.5194/acp-6-925-2006, 2006.

Schmid, O., Eimer, B., Hagen, D. E., and Whitefield, P. D.: Investigation of Volatility Method for Measuring Aqueous Sulfuric Acid on Mixed Aerosols, Aerosol Sci. Technol., 36, 877–889, doi:10.1080/02786820290038519, 2002.

Setyan, A., Zhang, Q., Merkel, M., Knighton, W. B., Sun, Y., Song, C., Shilling, J. E., Onasch, T. B., Herndon, S. C., Worsnop, D. R., Fast, J. D., Zaveri, R. A., Berg, L. K., Wiedensohler, A., Flowers, B. A., Dubey, M. K., and Subramanian, R.: Characterization of submicron particles influenced by mixed biogenic and anthropogenic emissions using high-resolution aerosol mass spectrometry: results from CARES, Atmos. Chem. Phys., 12, 8131–8156, doi:10.5194/acp-12-8131-2012, 2012.

Sievering, H., Gorman, E., Ley, T., Pszenny, A., Springer-Young, M., Boatman, J., Kim, Y., Nagamoto, C., and Wellman, D.: Ozone oxidation of sulfur in sea-salt aerosol particles during the Azores Marine Aerosol and Gas Exchange experiment, J. Geophys. Res., 100, 23075–23081, doi:10.1029/95jd01250, 1995.

Smith, M. H. and O'Dowd, C. D.: Observations of accumulation mode aerosol composition and soot carbon concentrations by means of a high-temperature volatility technique, J. Geophys. Res., 101, 19583–19591, doi:10.1029/95jd01750, 1996.

Spindler, G., Bruggemann, E., Gnauk, T., Grüner, A., Müller, K., and Herrmann, H.: A four-year size-segregated characterization study of particles PM_{10}, $PM_{2.5}$ and PM_1 depending on air mass origin at Melpitz, Atmos. Environ., 44, 164–173, doi:10.1016/j.atmosenv.2009.10.015, 2010.

Spindler, G., Gnauk, T., Grüner, A., Iinuma, Y., Müller, K., Scheinhardt, S., and Herrmann, H.: Size-segregated characterization of PM_{10} at the EMEP site Melpitz (Germany) using a five-stage impactor: a six year study, J. Atmos. Chem., 69, 127–157, doi:10.1007/s10874-012-9233-6, 2012.

Spindler, G., Grüner, A., Müller, K., Schlimper, S., and Herrmann, H.: Long-term size-segregated particle (PM_{10}, $PM_{2.5}$, PM_1) characterization study at Melpitz – influence of air mass inflow, weather conditions and season, J. Atmos. Chem., 70, 165–195, doi:10.1007/s10874-013-9263-8, 2013.

Stanier, C. O., Khlystov, A. Y., Chan, W. R., Mandiro, M., and Pandis, S. N.: A method for the in situ measurement of fine aerosol water content of ambient aerosols: The dry-ambient aerosol size spectrometer (DAASS), Aerosol Sci. Technol., 38, 215–228, doi:10.1080/02786820390229525, 2004.

Stier, P., Seinfeld, J. H., Kinne, S., and Boucher, O.: Aerosol absorption and radiative forcing, Atmos. Chem. Phys., 7, 5237–5261, doi:10.5194/acp-7-5237-2007, 2007.

Totlandsdal, A. I., Herseth, J. I., Bolling, A. K., Kubatova, A., Braun, A., Cochran, R. E., Refsnes, M., Ovrevik, J., and Lag, M.: Differential effects of the particle core and organic extract of diesel exhaust particles, Toxicol. Lett., 208, 262–268, doi:10.1016/j.toxlet.2011.10.025, 2012.

Tuch, T. M., Haudek, A., Müller, T., Nowak, A., Wex, H., and Wiedensohler, A.: Design and performance of an automatic regenerating adsorption aerosol dryer for continuous operation at monitoring sites, Atmos. Meas. Tech., 2, 417–422, doi:10.5194/amt-2-417-2009, 2009.

Turpin, B. J. and Lim, H.-J.: Species contributions to $PM_{2.5}$ mass concentrations: revisiting common assumptions for estimating organic mass, Aerosol Sci. Technol., 35, 302–610, doi:10.1080/02786820119445, 2001.

Ulbrich, I. M., Canagaratna, M. R., Zhang, Q., Worsnop, D. R., and Jimenez, J. L.: Interpretation of organic components from Positive Matrix Factorization of aerosol mass spectrometric data, Atmos. Chem. Phys., 9, 2891–2918, doi:10.5194/acp-9-2891-2009, 2009.

Wehner, B., Philippin, S., and Wiedensohler, A.: Design and calibration of a thermodenuder with an improved heating unit to measure the size-dependent volatile fraction of aerosol particles, J. Aerosol Sci., 33, 1087–1093, doi:10.1016/S0021-8502(02)00056-3, 2002.

Wehner, B., Petäjä, T., Boy, M., Engler, C., Birmili, W., Tuch, T., Wiedensohler, A., and Kulmala, M.: The contribution of sulfuric acid and non-volatile compounds on the growth of freshly formed atmospheric aerosols, Geophys. Res. Lett., 32, L17810, doi:10.1029/2005gl023827, 2005.

Wiedensohler, A., Birmili, W., Nowak, A., Sonntag, A., Weinhold, K., Merkel, M., Wehner, B., Tuch, T., Pfeifer, S., Fiebig, M., Fjäraa, A. M., Asmi, E., Sellegri, K., Depuy, R., Venzac, H., Villani, P., Laj, P., Aalto, P., Ogren, J. A., Swietlicki, E., Williams, P., Roldin, P., Quincey, P., Hüglin, C., Fierz-Schmidhauser, R., Gysel, M., Weingartner, E., Riccobono, F., Santos, S., Grüning, C., Faloon, K., Beddows, D., Harrison, R., Monahan, C., Jennings, S. G., O'Dowd, C. D., Marinoni, A., Horn, H.-G., Keck, L., Jiang, J., Scheckman, J., McMurry, P. H., Deng, Z., Zhao, C. S., Moerman, M., Henzing, B., de Leeuw, G., Löschau, G., and Bastian, S.: Mobility particle size spectrometers: harmonization of technical standards and data structure to facilitate high quality long-term observations of atmospheric particle number size distributions, Atmos. Meas. Tech., 5, 657–685, doi:10.5194/amt-5-657-2012, 2012.

Wu, Z., Poulain, L., Wehner, B., Wiedensohler, A., and Herrmann, H.: Characterization of the volatile fraction of laboratory-generated aerosol particles by thermodenuder-Aerosol Mass Spectrometer coupling experiments, J. Aerosol Sci., 40, 603–612, doi:10.1016/j.jaerosci.2009.03.007, 2009.

Zhang, Q., Jimenez, J. L., Canagaratna, M. R., Allan, J., Coe, H., Ulbrich, I., Alfarra, M. R., Takami, A., Middlebrook, A., Sun, Y. L., Dzepina, K., Dunlea, E., Docherty, K., Decarlo, P. F., Salcedo, D., Onasch, T. B., Jayne, J. T., Miyoshi, T., Shimono, A., Hatakeyama, S., Takegawa, N., Kondo, Y., Schneider, J., Drewnick, F., Borrmann, S., Weimer, S., Demerjian, K. L., Williams, P., Bower, K. N., Bahreini, R., Cottrell, L., Griffin, R. J., Rautiainen, J., Sun, J. Y., Zhang, Y. H., and Worsnop, D. R.: Ubiquity and dominance of oxygenated species in organic aerosols in anthropogenically-influenced Northern Hemisphere midlatitudes, Geophys. Res. Lett., 34, L13801, doi:10.1029/2007GL029979, 2007.

Zhao, Y. L. and Gao, Y.: Acidic species and chloride depletion in coarse aerosol particles in the US east coast, Sci. Total Environ., 407, 541–547, doi:10.1016/j.scitotenv.2008.09.002, 2008.